Stationary entanglement between two nanomechanical oscillators induced by Coulomb interaction*

Qin Wu(吴琴)[1,2], Yin Xiao(肖银)[1], and Zhi-Ming Zhang(张智明)[1,†]

[1] *Guangdong Provincial Key Laboratory of Nanophotonic Functional Materials and Devices (SIPSE), Guangdong Provincial Key Laboratory of Quantum Engineering and Quantum Materials, South China Normal University, Guangzhou* 510006, *China*

[2] *School of Information Engineering, Guangdong Medical University, Dongguan* 523808, *China*

(Received 4 July 2015; revised manuscript received 20 October 2015; published online 30 November 2015)

We propose a scheme for entangling two nanomechanical oscillators by Coulomb interaction in an optomechanical system. We find that the steady-state entanglement of two charged nanomechanical oscillators can be obtained when the coupling between them is stronger than a critical value which relies on the detuning. Remarkably, the degree of entanglement can be controlled by the Coulomb interaction and the frequencies of the two charged oscillators.

Keywords: entanglement, Coulomb interaction, optomechanical system

PACS: 42.50.Wk, 46.80.+j, 41.20.Cv **DOI:** 10.1088/1674-1056/25/1/014203

1. Introduction

Cavity optomechanics has sparked the interest of a vast scientific community over the past few years due to its distinct applications, such as the high-sensitivity detection of tiny mass, force, and displacement.[1–4] In a typical optomechanical system, a movable mirror couples the cavity field by the radiation pressure, and this coupling can lead to many remarkable effects, for example, the optomechanically induced transparency (OMIT),[5–11] the quantum ground state cooling of the nanomechanical oscillators,[12,13] the entanglement between cavity modes and/or mechanical modes,[14–23] and the squeezed states of light or mechanical modes.[24–26]

Entanglement is one of the most striking properties of quantum mechanics and has become a significant resource for quantum information processing. Although quantum mechanics has been proven to be highly successful in explaining physics at microscopic and subatomic scales, its validity at macroscopic scales is still debated. Over recent decades, thanks to the theoretical study and technological progress, it has now been possible to obtain entanglement in mesoscopic and even macroscopic systems. In addition to the theoretical proposals[14–17] that predict entanglement between a mechanical oscillator and a cavity field, the recent experimental realization[18] of entanglement between the motion of a mechanical oscillator and a propagating microwave in an electromechanical circuit makes optomechanical system a promising platform for generating macroscopic entanglement. Moreover, entanglement between mechanical oscillators can also be obtained by use of the squeezed input optical field,[27–29] the cascaded cavity coupling,[30] and the conditional quantum measurements.[31,32] In fact, entangled optomechanical systems have potential profitable application in realizing quantum communication networks, in which the mechanical modes play the vital role of local nodes where quantum information can be stored and retrieved, and optical modes carry the information between the nodes. This allows the implementation of CV quantum teleportation,[33,34] quantum telecloning,[35] and entanglement swapping.[36]

In this work, we investigate the entanglement in an optomechanical cavity coupled to an external nanomechanical oscillator (NMO) via Coulomb interaction. Using logarithmic negatively as an entanglement measure, we show that the two charged NMOs are entangled in the steady state through introducing the Coulomb coupling. The generated NMO–NMO entanglement is strongly dependent on the Coulomb coupling strength and the frequencies of the two charged mirrors. In addition, we also show the robustness of the entanglement to temperature at different pump power.

Different from the conventional optomechanical systems[37,38] where the entanglement between two movable mechanical oscillators is generated by the inner cavity modes or induced by the external atoms, the entanglement between the two charged NMOs in our scheme is created by Coulomb interaction. Moreover, compared with the conventional methods, the Coulomb coupling has important advantages, for example, the range of the interaction distance is from nanometer to meter,[39,40] the strength can be controlled by the bias

*Project supported by the Major Research Plan of the National Natural Science Foundation of China (Grant No. 91121023), the National Natural Science Foundation of China (Grant Nos. 61378012, 60978009, and 11574092), the Specialized Research Fund for the Doctoral Program of Higher Education of China (Grant No. 20124407110009), the National Basic Research Program of China (Grant Nos. 2011CBA00200 and 2013CB921804), and the Program for Changjiang Scholar and Innovative Research Team in University, China (Grant No. IRT1243).

†Corresponding author. E-mail: zmzhang@scnu.edu.cn

© 2016 Chinese Physical Society and IOP Publishing Ltd

voltage,[41] and it can also be applied to couple different kinds of charged objects at different frequencies.[42]

The rest of this paper is organized as follows. In Section 2, we present the model under study and the analytical expressions of the optomechanical system, and derive the quantum Langevin equations and the steady state of the system. In Section 3, we quantify the entanglement properties of the two charged NMOs by using the logarithmic negativity. Finally we draw our conclusions in Section 4.

2. Model and solution

As sketched in Fig. 1, our system consists of a high-quality Fabry–Pérot cavity containing a fixed mirror and a movable mirror NMO_1. NMO_1 is charged by the bias gate voltage V_1 and subject to the Coulomb force due to another charged NMO_2 with the bias gate voltage $-V_2$. The optomechanical cavity of the length L is driven by one strong pump field ε_p from the left side of the cavity. The output field is represented by ε_out, q_1 and q_2 represent the small displacements of NMO_1 and NMO_2 from their equilibrium positions, with r_0 the equilibrium distance between the two NMOs. Then, the Hamiltonian in the rotating frame at frequency of the pump field ω_p can be given by

$$\begin{aligned} H &= \hbar\Delta_\mathrm{c} c^\dagger c + \frac{\hbar\omega_1}{2}(p_1^2+q_1^2) + \frac{\hbar\omega_2}{2}(p_2^2+q_2^2) \\ &\quad -\hbar g c^\dagger c q_1 + \hbar\lambda q_1 q_2 + \mathrm{i}\hbar\varepsilon_\mathrm{p}(c^\dagger - c), \end{aligned} \tag{1}$$

where the first term is for the single-mode cavity field with frequency ω_c and annihilation (creation) operator c ($c^\dagger$), and $\Delta_\mathrm{c} = \omega_\mathrm{c} - \omega_\mathrm{p}$ is the detuning of the pump field from the bare cavity. The second (third) term describes the vibration of the charged NMO_1 (NMO_2) with frequency ω_1 (ω_2), effective mass m_1 (m_2), position operator q_1 (q_2) and momentum operator p_1 (p_2).[43] The fourth term describes the coupling between NMO_1 and the cavity field with the coupling strength $g = (\omega_\mathrm{c}/L)\sqrt{\hbar/m\omega_1}$, where L is the cavity length. The fifth term presents the Coulomb coupling between the charged NMO_1 and NMO_2 with the Coulomb coupling strength $\lambda = (C_1V_1C_2V_2)/(2\pi\hbar\varepsilon_0 r_0^3)$,[41,42] where the NMO_1 and NMO_2 take the charges $Q_1 = C_1V_1$ and $Q_2 = -C_2V_2$, with $C_1(C_2)$ and $V_1(-V_2)$ being the capacitance and the voltage of the bias gate, respectively. The last term in Eq. (1) describes the interactions between the cavity field with the input field. The strong pump field possesses the frequency ω_p and the amplitude $\varepsilon_\mathrm{p} = \sqrt{2\kappa P/\omega_\mathrm{p}}$, where P is the power of the pump field and κ is the cavity decay rate.

Considering photon losses from the cavity and the Brownian noise from the environment, we may describe the dynamics of the system governed by Eq. (1) using the following nonlinear quantum Langevin equations:[43]

$$\begin{aligned} \dot{q}_1 &= \omega_1 p_1, \\ \dot{p}_1 &= -\omega_1 q_1 - \gamma_1 p_1 + g c^\dagger c - \lambda q_2 + \xi_1, \\ \dot{q}_2 &= \omega_2 p_2, \\ \dot{p}_2 &= -\omega_2 q_2 - \gamma_2 p_2 - \lambda q_1 + \xi_2, \\ \dot{c} &= -(\kappa + \mathrm{i}\Delta_\mathrm{c})c + \mathrm{i}gcq_1 + \varepsilon_\mathrm{p} + \sqrt{2\kappa}c_\mathrm{in}, \end{aligned}$$

where γ_1 (γ_2) is the decay rate for NMO_1 (NMO_2). The quantum Brownian noise ξ_1 (ξ_2) comes from the coupling between NMO_1 (NMO_2) and its own environment with correlation function[44]

$$\langle \xi(t)\xi'(t)\rangle \simeq \gamma_\mathrm{m}(2\bar{n}+1)\delta(t-t'),$$

where $\bar{n} = [\exp(\hbar\omega_\mathrm{m}/k_\mathrm{B}T) - 1]^{-1}$ is the mean number of thermal excitation with k_B being the Boltzmann constant, c_in is the input vacuum noise operator with nonzero correlation function[44]

$$\langle c_\mathrm{in}(t)c_\mathrm{in}^\dagger(t)\rangle = \delta(t-t').$$

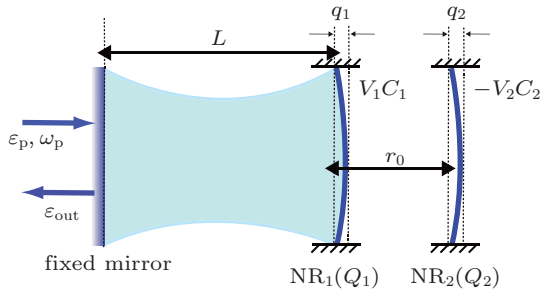


Fig. 1. (color online) Schematic diagram of the system.

From the Langevin equations above, we can obtain the steady-state mean-values as

$$\begin{aligned} p_{1\mathrm{s}} &= 0, \\ p_{2\mathrm{s}} &= 0, \\ q_{1\mathrm{s}} &= \frac{g|c_\mathrm{s}|^2}{\omega_1 - \dfrac{\lambda^2}{\omega_2}}, \\ q_{2\mathrm{s}} &= \frac{-\lambda}{\omega_2} q_{1\mathrm{s}}, \\ c_\mathrm{s} &= \frac{\varepsilon_\mathrm{p}}{\kappa + \mathrm{i}\Delta}, \end{aligned}$$

where $\Delta = \Delta_\mathrm{c} - gq_{1\mathrm{s}}$ is the effective cavity detuning.

We can rewrite each Heisenberg operator as its steady-state mean-value plus an additional fluctuation operator with zero-mean value, $c = c_\mathrm{s} + \delta c$, $q_i = q_{i\mathrm{s}} + \delta q_i, p_i = p_{i\mathrm{s}} + \delta p_i$ ($i = 1,2$). For generating optomechanical entanglement the input power is usually very large, which means $|c_\mathrm{s}| \gg 1$, so we can ignore some small quantity and get the linearized Langevin equations

$$\delta\dot{q}_1 = \omega_1 \delta p_1,$$

$$\begin{aligned}
\delta\dot{p}_1 &= -\omega_1\delta q_1 - \gamma_1\delta p_1 + G(\delta c + \delta c^\dagger) - \lambda\delta q_2 + \xi_1,\\
\delta\dot{q}_2 &= \omega_2\delta p_2,\\
\delta\dot{p}_2 &= -\omega_2\delta q_2 - \gamma_2\delta p_2 - \lambda\delta q_1 + \xi_2,\\
\delta\dot{c} &= -(\kappa + \mathrm{i}\Delta)\delta c + \mathrm{i}G\delta q_1 + \sqrt{2\kappa}c_{\mathrm{in}},
\end{aligned} \tag{2}$$

where $G = gc_{\mathrm{s}}$ is the effective coupling strength.

3. Entanglement

In this section, we study the NMO–NMO entanglement and analyze how the degree of entanglement depends on the Coulomb interaction and the frequencies of the two charged NMOs. We also investigate the robustness of the entanglement against temperature.

In order to investigate the optomechanical entanglement, it is more convenient to use the quadratures operators defined by $\delta X = (\delta c + \delta c^\dagger)/\sqrt{2}$ and $\delta Y = (\delta c - \delta c^\dagger)/\mathrm{i}\sqrt{2}$, and the corresponding Hermitian input noise operators $X_{\mathrm{in}} = (c_{\mathrm{in}} + c_{\mathrm{in}}^\dagger)/\sqrt{2}$ and $Y_{\mathrm{in}} = (c_{\mathrm{in}} - c_{\mathrm{in}}^\dagger)/\mathrm{i}\sqrt{2}$. Then equation (2) can be rewritten as the matrix form

$$\dot{\boldsymbol{u}} = \boldsymbol{A}\boldsymbol{u}(t) + \boldsymbol{n}(t), \tag{3}$$

in which the transposes of the column vectors $\boldsymbol{u}(t)$ and $\boldsymbol{n}(t)$ can be expressed as

$$\begin{aligned}
\boldsymbol{u}^{\mathrm{T}}(t) &= (\delta q_1(t), \delta p_1(t), \delta q_2(t), \delta p_2(t), \delta X(t), \delta Y(t)),\\
\boldsymbol{n}^{\mathrm{T}}(t) &= (0, \xi_1(t), 0, \xi_2(t), \sqrt{2\kappa}X^{\mathrm{in}}(t), \sqrt{2\kappa}Y^{\mathrm{in}}(t)),
\end{aligned} \tag{4}$$

and the matrix $\boldsymbol{A}$ is

$$\boldsymbol{A} = \begin{pmatrix}
0 & \omega_1 & 0 & 0 & 0 & 0\\
-\omega_1 & -\gamma_1 & -\lambda & 0 & G_{\mathrm{m}} & 0\\
0 & 0 & 0 & \omega_2 & 0 & 0\\
-\lambda & 0 & -\omega_2 & -\gamma_2 & 0 & 0\\
0 & 0 & 0 & 0 & -\kappa & \Delta\\
G_m & 0 & 0 & 0 & -\Delta & -\kappa
\end{pmatrix},$$

where the effective optomechanical coupling $G_{\mathrm{m}} = \sqrt{2}gc_{\mathrm{s}}$. When the system is stable, it reaches a unique steady state, independently of the initial condition. Since the quantum noises $\xi_{1(2)}$ and c_{in} are zero-mean quantum Gaussian noises and the dynamics is linearized, the quantum steady state for the fluctuations is a zero-mean bipartite Gaussian state.

The solution of Eq. (3) can be expressed as

$$\boldsymbol{u}(t) = \boldsymbol{M}(t)\boldsymbol{u}(0) + \int_0^t \mathrm{d}t'\boldsymbol{M}(t')\boldsymbol{n}(t-t'), \tag{5}$$

where $\boldsymbol{M}(t) = \exp(\boldsymbol{A}t)$. The system is stable only if the real parts of all the eigenvalues of matrix $\boldsymbol{A}$ are negative, which can be derived by applying the Routh–Hurwitz criterion.[45] We will choose the parameters so that the system is subsequently in a steady state. We define $V_{ij} = \langle u_i(\infty)u_j(\infty) + u_j(\infty)u_i(\infty)\rangle/2$, which is a 6×6 correlation matrix (CM).[46–48] Here, $\boldsymbol{u}^{\mathrm{T}}(\infty) = (\delta q_1(\infty), \delta p_1(\infty), \delta q_2(\infty), \delta p_2(\infty), \delta X(\infty), \delta Y(\infty))$ is the vector of the fluctuations operators at the steady state. When the system is stable ($t\to\infty$), we obtain

$$V_{ij} = \sum_{k,l}\int_0^\infty \mathrm{d}t\int_0^\infty \mathrm{d}t' M_{ik}(t)M_{jl}(t')\Phi_{kl}(t-t'), \tag{6}$$

where $\Phi_{kl}(t-t') = (\langle n_k(t)n_l(t') + n_l(t')n_k(t)\rangle)/2$ is the steady-state noise CM. When the stability conditions are satisfied, the steady-state CM satisfies a Lyapunov equation

$$\boldsymbol{A}\boldsymbol{V} + \boldsymbol{V}\boldsymbol{A}^{\mathrm{T}} = -\boldsymbol{D}, \tag{7}$$

where $\boldsymbol{D} = \mathrm{diag}[0, \gamma_1(2\bar{n}_1+1), 0, \gamma_2(2\bar{n}_2+1), \kappa, \kappa]$ and $\bar{n}_j = [\exp(\hbar\omega_j/k_{\mathrm{B}}T) - 1]^{-1}(j = 1,2)$ is the mean thermal excitation number. We can straightforwardly have the solution of the CM with Eq. (7). However, the explicit expression is too complicated and will not be reported here.

Now, we examine the NMO–NMO entanglement of this optomechanical system. For this purpose, we consider the entanglement of the bipartite subsystems that can be traced over the remaining degrees of freedom. This bipartite entanglement will be quantified by using the logarithmic negativity

$$E_{\mathrm{N}} = \max[0, -\ln 2\eta^-], \tag{8}$$

where $\eta^- \equiv 2^{-1/2}[\Sigma(\boldsymbol{V}_{\mathrm{bp}}) - \sqrt{\Sigma(\boldsymbol{V}_{\mathrm{bp}})^2 - 4\det(\boldsymbol{V}_{\mathrm{bp}})}]^{1/2}$ is the lowest symplectic eigenvalue of the partial transpose of the 4×4 CM, V_{bp}, associated with the selected bipartition, obtained by disregarding the rows and columns of the uninteresting mode,

$$\boldsymbol{V}_{\mathrm{bp}} = \begin{pmatrix} \boldsymbol{B} & \boldsymbol{C}\\ \boldsymbol{C}_{\mathrm{T}} & \boldsymbol{B}' \end{pmatrix}, \tag{9}$$

and $\Sigma(\boldsymbol{V}_{\mathrm{bp}}) \equiv \det\boldsymbol{B} + \det\boldsymbol{B}' - 2\det\boldsymbol{C}$.

For simplicity, we choose all the parameters of the two charged NMOs to be the same, i.e., $\omega_1 = \omega_2 = \omega_{\mathrm{m}}$, $\gamma_1 = \gamma_2 = \gamma_{\mathrm{m}}$. In order to obtain a significant amount of entanglement, we have made a careful analysis in a wide parameter range and found the system parameters, as shown in Table 1, which are very close to that of performed optomechanical experiments.[49,50] We numerically display the entanglement of the two movable mirrors in Figs. 2–4.

Table 1. The parameters used in our numerical calculations which are based on the experiment conditions.[49,50]

Paramter	Symbol	Value
Mechanical mass	m	5 ng
Mechanical frequency	$\omega_{\mathrm{m}}/2\pi$	100 MHz
Mechanical damping rate	$\gamma_{\mathrm{m}}/2\pi$	100 Hz
Cavity length	L	1 mm
Cavity-field wavelength	λ_0	810 nm
Optical damping rate	κ	88.1 MHz

In Fig. 2, we plot the logarithmic negativity E_N versus the normalized detuning Δ/ω_m at temperature $T = 4$ mK and driving power $P = 50$ mW for three values of the Coulomb coupling strength $\lambda = 0.3\omega_m$ (solid line), $\lambda = 0.5\omega_m$ (dashed line), and $\lambda = 0.9\omega_m$ (dashed-dotted line). It can be clearly seen that the NMO–NMO entanglement is enhanced with the increase of the coupling parameter λ. In the case of $\lambda = 0.3\omega_m$, the optimal entanglement remains near $\Delta/\omega_m = 1$ and for $\lambda = 0.9\omega_m$ it is shifted towards lower detuning value around $\Delta/\omega_m = 0.5$. More importantly, with increasing the NMO–NMO coupling, the range of the entanglement between the two NMOs can be broadened, i.e., from $\Delta/\omega_m \in [0.6, 1.4]$ (solid line) to $\Delta/\omega_m \in [0.2, 1.6]$ (dashed-dotted line). The broader the effective detuning, the more easily it is realized in experiments. From Fig. 2, we can find that the main reason for formation of entanglement between the two nanomechanical oscillators is the existence of Coulomb coupling. The numerical results also show that it is not possible to entangle the two NMOs if there is not the Coulomb coupling.

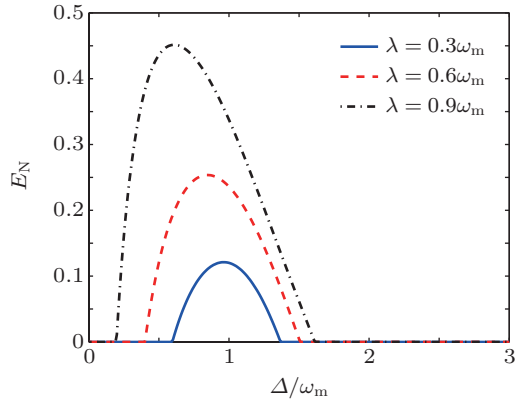


Fig. 2. (color online) Plot of the logarithmic negativity as a function of the normalized detuning Δ/ω_m.

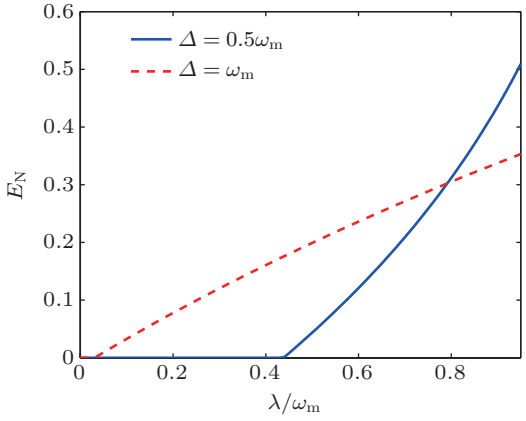


Fig. 3. (color online) Plot of the logarithmic negativity as a function of the NMO–NMO coupling strength λ/ω_m.

To further explore the effect of NMO–NMO coupling strength on the entanglement of the two charged NMOs, we plot in Fig. 3 the logarithmic negativity E_N versus λ/ω_m at temperature $T = 4$ mK and driving power $P = 50$ mW. It is obvious that the two oscillators are unentangled below a critical coupling strength λ_c and the NMO–NMO entanglement increases nearly linearly with λ in the range $\lambda \in [\lambda_c, 0.95\omega_m]$. We find the critical coupling strength $\lambda_{c1} = 0.03\omega_m$ for the case of $\Delta = \omega_m$ (dashed line), and $\lambda_{c2} = 0.43\omega_m$ for $\Delta = 0.5\omega_m$ (solid line). More interestingly, the increase rate in the case of $\Delta = \omega_m$ is smaller than that in the case of $\Delta = 0.5\omega_m$.

Figure 4 shows the robustness of the entanglement against the environmental temperature with fixed Coulomb coupling strength $\lambda = 0.6\omega_m$ and detuning $\Delta = \omega_m$ while varying the power of the driving laser. We find that the robustness of NMO–NMO entanglement with respect to the environment temperature is enhanced when we increase the laser power.

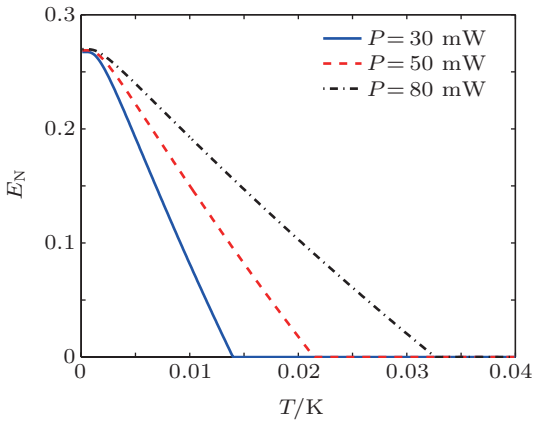


Fig. 4. (color online) Plot of the logarithmic negativity versus the environment temperature.

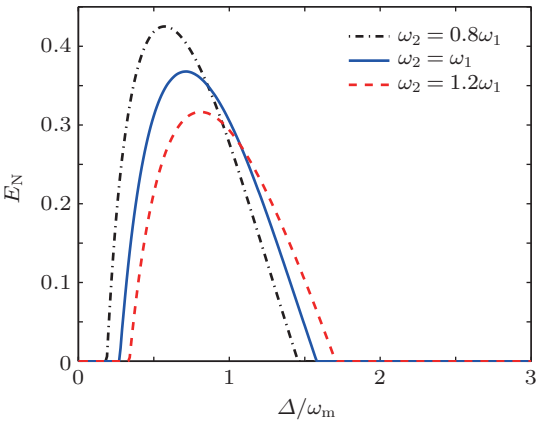


Fig. 5. (color online) Plot of the logarithmic negativity as a function of the normalized detuning Δ/ω_m when the frequencies of two oscillators are different.

In practice, it is hard to achieve two identical NMOs in experiments. For this reason, we plot in Fig. 5 the numerical simulation of the NMO–NMO entanglement when the two charged NMOs have different frequencies ($\omega_1 \neq \omega_2$), where we set $T = 4$ mK, $P = 50$ mW, and $\lambda = 0.6\omega_m$. In order to make a comparison, we also plot E_N when $\omega_1 = \omega_2$ (solid curve). This figure shows that the maximal entanglement between the two charged NMOs is obtained when the

frequency of NMO_2 is smaller than the frequency of NMO_1, i.e., $\omega_2 = 0.8\omega_1$ (dash-dotted curve). When $\omega_2 = 1.2\omega_1$, the maximal entanglement is decreased and the optimal entanglement is shifted towards higher detuning value (dashed curve). The above discussion implies that we can control the value of NMO–NMO entanglement and the optimal entanglement occurrence through adjusting the Coulomb interaction and frequencies of the two charged NMOs.

4. Conclusion

In conclusion, we have analyzed the NMO–NMO entanglement in an optomechanical system with two charged NMOs. We show that due to the Coulomb interaction between the two NMOs, they can be entangled. We also find that the generated entanglement can be controlled by adjusting the Coulomb coupling strength and the frequencies of the two charged NMOs: i) The entanglement between the two charged NMOs is enhanced with increasing the Coulomb coupling strength λ. ii) The degree of NMO–NMO entanglement is increased when the frequency of NMO_2 is smaller than the frequency of NMO_1 ($\omega_2 > \omega_1$), and is decreased when $\omega_2 < \omega_1$. iii) The points for the optimal entanglement will be shifted to the left for $\omega_2 < \omega_1$ and to the right for $\omega_2 > \omega_1$. Besides, we show that increasing the driving power leads to much more robust entanglement against temperature.

References

[1] Kippenberg T J and Vahala K J 2008 *Science* **321** 1172
[2] Marquardt F and Girvin S M 2009 *Physics* **2** 40
[3] Verlot P, Tavernarakis A, Briant T, Cohadon P F and Heidmann A 2010 *Phys. Rev. Lett.* **104** 133602
[4] Mahajan S, Kumar T, Bhattacherjee A B and ManMohan 2013 *Phys. Rev. A* **87** 013621
[5] Huang S and Agarwal G S 2011 *Phys. Rev. A* **83** 043826
[6] Han Y, Cheng J and Zhou L 2011 *J. Phys. B: At. Mol. Opt. Phys.* **44** 165505
[7] Ma Y H and Zhou L 2013 *Chin. Phys. B* **22** 024204
[8] Karuza M, Biancofiore C, Bawaj M, Molinelli C, Galassi M, Natali R, Tombesi P, Diuseppe G and Vitali D 2013 *Phys. Rev. A* **88** 013804
[9] Shu J 2011 *Chin. Phys. Lett.* **28** 104203
[10] Yan X B, Yang L, Tian X D, *et al.* 2014 *Acta Phys. Sin.* **63** 204201 (in Chinese)
[11] Yan X B, Gu K H, Fu C B, *et al.* 2014 *Chin. Phys. B* **23** 114201
[12] Rocheleau T, Ndukum T, Machlin C, Hertzberg J, Clerk A and Schwab K 2010 *Nature* **463** 72
[13] Miao H, Danilishin S, Müller-Ebhardt H and Chen Y 2010 *New J. Phys.* **12** 083032
[14] Vitali D, Gigan S, Ferreira A, Böhm H R, Tombesi P, Guerreiro A, Vedral V, Zeilinger A and Aspelmeyer M 2007 *Phys. Rev. Lett.* **98** 030405
[15] Genes C, Mari A, Tombesi P and Vitali D 2008 *Phys. Rev. A* **78** 032316
[16] Akram U, Munro W, Nemoto K and Milburn G J 2012 *Phys. Rev. A* **86** 042306
[17] Mi X W, Bai J X and Song K H 2013 *Eur. Phys. J. D* **67** 115
[18] Palomaki T A, Teufel J D, Simmonds R W and Lehnert K W 2013 *Science* **342** 710
[19] Joshi C, Akram U and Milburn G J 2014 *New J. Phys.* **16** 023009
[20] Liao J Q, Wu Q Q and Nori F 2014 *Phys. Rev. A* **89** 014302
[21] Ghobadi R, Kumar S, Pepper B, Bouwmeester D, Lvovsky A I and Simon C 2014 *Phys. Rev. Lett.* **112** 080503
[22] Ge W C, Al-Amri M, Nha H and Zubairy M S 2013 *Phys. Rev. A* **88** 022338
[23] Zheng Q and Zhang D 2013 *Chin. Phys. Lett.* **30** 024213
[24] Woolley M J, Doherty A C, Milburn G J and Schwab K C 2008 *Phys. Rev. A* **78** 062303
[25] Sete E A and Eleuch H 2012 *Phys. Rev. A* **85** 043824
[26] Asjad M, Agarwal G S, Kim M S, Tombesi P, Di Giuseppe G and Vitali D 2014 *Phys. Rev. A* **89** 023849
[27] Pinard M, Dantan A, Vitali D, Arcizet O, Briant T and Heidmann A 2005 *Europhys. Lett.* **72** 747
[28] Zhang J, Peng K and Braunstein S L 2003 *Phys. Rev. A* **68** 013808
[29] Huang S and Agarwal G S 2009 *New J. Phys.* **11** 103044
[30] Tan H, Buchmann L F, Seok H and Li G 2013 *Phys. Rev. A* **87** 022318
[31] Børkje K, Nunnenkamp A and Girvin S M 2011 *Phys. Rev. Lett.* **107** 123601
[32] Woolley M J and Clerk A A 2013 *Phys. Rev. A* **87** 063846
[33] Mancini S, Vitali D and Tombesi P 2003 *Phys. Rev. Lett.* **90** 137901
[34] Pirandola S, Mancini S, Vitali D and Tombesi P 2003 *Phys. Rev. A* **68** 062317
[35] Pirandola S, Mancini S, Vitali D and Tombesi P 2004 *J. Mod. Opt.* **51** 901
[36] Pirandola S, Vitali D, Tombesi P and Lloyd S 2006 *Phys. Rev. Lett.* **97** 150403
[37] Zhou L, Han Y, Jing J T and Zhang W P 2011 *Phys. Rev. A* **83** 052117
[38] Hartmann M J and Plenio M B 2008 *Phys. Rev. Lett.* **101** 200503
[39] Löw U, Emery V J and Fabricius K 1994 *Phys. Rev. Lett.* **72** 1918
[40] Bohm D and Pines D 1953 *Phys. Rev.* **92** 609
[41] Ma P C, Zhang J Q, Xiao Y, Feng M and Zhang Z M 2014 *Phys. Rev. A* **90** 043825
[42] Hensinger W K, Utami D W, Goan H S, Schwab K, Monroe C and Milburn G J 2005 *Phys. Rev. A* **72** 041405(R)
[43] Agarwal G S and Huang M 2012 *Phys. Rev. A* **85** 021801(R)
[44] Genes C, Vitali D, Tombei D, Gigan S and Aspelmeyer M 2008 *Phys. Rev. A* **77** 033804
[45] DeJesus E X and Kaufman C 1987 *Phys. Rev. A* **35** 5288
[46] Adesso G and Illuminati F 2007 *J. Phys. A* **40** 7821
[47] Weedbrook C, Pirandola S, Garcia-Patrón R, Cerf N J, Ralph T C, Shapiro J H and Lloyd S 2012 *Rev. Mod. Phys.* **84** 621
[48] Olivares S 2012 *Eur. Phys. J. Special Topics* **203** 3
[49] Schliesser A, Riviere R, Anetsberger G, Arcizet O and Kippenberg T J 2008 *Nat. Phys.* **4** 415
[50] Gigan S, Böhm H R, Paternostro M, Blaser F, Langer G, Hertzberg J B, Schwab K C, Bäuerle D, Aspelmeyer M and Zeilinger A 2006 *Nature* **444** 67